Dosimetric Measurement of Scattered Radiation From Dental Implants in Simulated Head and Neck Radiotherapy

Russell Wang, DDS, MSD*/Kunjan Pillai, PhD**/Paul K. Jones, PhD***

The purpose of this study was to examine the dose enhancement at bone-implant interfaces from scattered radiation during simulated head and neck radiotherapy. Three cylindric implant systems with different compositions (pure titanium, titanium-aluminum-vanadium alloy, titanium coated with hydroxyapatite) and a high gold content transmandibular implant system (gold-copper-silver alloy) were studied. Extruded lithium fluoride single crystal chips were used as thermoluminescent material to measure radiation dose enhancement at 0, 1, and 2 mm from the bone-implant interface. The relative doses in buccal, lingual, mesial, and distal directions were also recorded and compared. The results indicated that the highest dose enhancement occurred at a distance of 0 mm from the bone-implant interface for all the implant systems studied. The transmandibular implants had higher scattered radiation than other groups at 0 mm and at 1 mm from the bone-implant interface. There was no significant difference of dose enhancement between buccal, lingual, mesial, and distal directions. Titanium implants coated with hydroxyapatite demonstrated the best results under the simulated irradiation.
(INT J ORAL MAXILLOFAC IMPLANTS 1998;13:197–203)

Key words: bone-implant interface, head and neck radiotherapy, scattered radiation, thermoluminescent dosimetry (TLD), titanium implant, transmandibular implant system

The use of dental implants to restore speech, esthetics, and masticatory function for partially and completely edentulous patients has increased dramatically in recent years. An estimated 300,000 dental implants were placed in the United States in 1992.[1] Many dental implants are placed in patients who are 50 years of age or older, an age group most likely to need dental implants or prostheses and to be prone to have cancer. It is a virtual certainty that many of the patients now receiving dental implants will one day require radiotherapy should they develop head and neck cancer. Therefore, it is important to assess the relationship between dental implants and radiation therapy as new implant systems for clinical applications are evolving.

The purpose of radiotherapy is to eradicate a tumor by exposing it to ionizing radiation. Ideally, radiotherapy will be well tolerated by surrounding structures, while in practice, some degree of transient or permanent tissue damage invariably occurs. In curative radiotherapy, the total radiation dose is high, and the treatment is usually prolonged and physically taxing.

Manifestations of oral complications from head and neck radiotherapy include xerostomia, loss of taste, changes in oral microflora and salivary chemistry, mucositis, glossitis, radiation caries, salivary dysfunction, dysphagia, muscle fibrosis, and tissue necrosis.[2,3] Osteoradionecrosis, correlated to high radiation doses, is a more severe complication that is difficult to treat.[4] A strong correlation has been documented between osteoradionecrosis and high-dose irradiation.[5–9]

*Assistant Professor, Department of Restorative Dentistry, School of Dentistry, Case Western Reserve University, Cleveland, Ohio.

**Assistant Professor, Division of Radiation Oncology, School of Medicine, Case Western Reserve University, Cleveland, Ohio.

***Associate Professor, Department of Epidemiology and Biostatistics, School of Medicine, Case Western Reserve University, Cleveland, Ohio.

Reprint requests: *Dr Russell Wang, Department of Restorative Dentistry, School of Dentistry, Case Western Reserve University, 10900 Euclid Avenue, Cleveland, Ohio 44106-4905. E-mail: rxw26@po.cwru.edu*

High-energy electron or photon beams are frequently used in the treatment of head and neck cancer. Often these treatments are delivered to a volume of tissue that contains heterogeneous media such as soft tissues, bone, teeth, or metal crowns. The presence of metallic crowns or dental implants in the radiation field may result in dose enhancement at the tissue-metal interface. The ionizing radiation interacts with the atoms of the metal, liberating and setting into motion electrons from within the metal. The adverse effects caused by scattered radiation from metal restorations such as gold crowns, especially those attributed to dosage, are often seen clinically and have been reported in the literature.[10–16] There is some concern that dental implant patients may have a higher risk of developing osteoradionecrosis resulting from head and neck radiotherapy, because of increased scattered radiation around implants.

Mian et al[17] examined the backscatter radiation on flat, commercially pure titanium (cpTi) disks in vitro using the ionization chamber method. The results showed that a backscatter factor at the substitute bone-titanium interface was about 15% with high energy 6 MeV x-ray irradiation. A slight decrease in the backscatter factor was obtained with an increase in the mean photon energy, such as 25 MeV x-ray irradiation. The results obtained from samples irradiated with cobalt 60 gamma ray were similar to those irradiated with 6 MeV x-rays. Wang et al[18] evaluated titanium-aluminum-vanadium (Ti-6A1-4V), high gold content alloy, and cpTi implant materials using 6 MeV and 10 MeV x-ray irradiation. The characteristics of backscatter radiation were similar with pure Ti and with Ti-6A1-4V implant disks. The high gold content of transmandibular implant material had a much higher degree of backscatter radiation. Backscattering decreased significantly when the measurements were conducted at 1, 2, and 3 mm away from the bone-implant interfaces.

The drawback in the previous studies is that flat metal disk samples are considerably different in size and shape from clinical dental implants. Therefore, the total amount of scattered radiation from a flat disk measured by the ionization chamber method may be different if the radiation dose were detected from a cylindrical implant surface. The advantage of the ionization chamber method is that measurements are very precise. Less than 0.1% errors were found between repeated measurements of scattered radiation in a previous study.[18] The disadvantage of this method is that the chamber is too large to be adapted properly in a curved mandible next to a root-form implant.

The purpose of this investigation was to determine the amount of scattered radiation at bone-implant interfaces from cylindric implant systems using the thermoluminescent dosimetry method.

The objectives of this investigation were to determine *(1)* the amount of scattered radiation from four implant systems irradiated with 6 MeV x-ray; *(2)* the effect of scattered radiation on buccal, lingual, mesial, and distal directions from four implant systems; and *(3)* the effect of scattered radiation on three bone-implant interfaces.

A Simplified Theory of the Thermoluminescent Dosimetry. The thermoluminescent dosimetry (TLD) method was introduced in the 1960s to measure ionizing radiation.[19] Thermoluminescent phosphor such as lithium fluoride (LiF) or calcium fluoride (CaF_2) can emit light and release previously absorbed radiation energy upon being moderately heated. LiF is the most commonly used material in thermoluminescent dosimetry. It has been successfully used to measure patients' therapeutic radiation exposure in some clinical situations.[20,21] LiF single crystal powder can be annealed and pressed into small pieces as TLD material to precisely measure radiation dose. A small TLD chip with a volume of 1 mm^3 or less can be made, which would be applicable to measure scattered radiation from dental implants during radiotherapy.

A hypothetical energy diagram of a crystal exhibiting thermoluminescence, resulting from ionization is illustrated in Figs 1a to 1c. Figure 1a represents the virgin crystal during exposure. Ionizing radiation releases an electron from the valence band to the conduction band, leaving a hole in the valence band. The electron and the hole move through the crystal until they recombine or are trapped in the metastable states shown. These metastable states are presumed to be associated with such defects in the crystal as impurity sites. There are then two possible ways by which a TL photon is emitted. As the crystal is heated, sufficient energy may be given to the electron to raise it to the conduction band (Fig 1b). This electron may wander around until it recombines with the trapped hole, and thus a TL photon is emitted. Or, the hole trap may be less stable than the electron trap (Fig 1c). The hole receives sufficient energy to wander until it recombines with the trapped electron, and again a TL photon is emitted. Since the two possibilities are similar, it is convenient to consider only the first (Fig 1b).

The energy gap, E, is related to the temperature needed to release the electron and thus produce the thermoluminescence. In a practical situation, many trapped electrons and holes are produced. As a crystal is heated, the probability of releasing any particular electron is increased, and at some temperature there is a virtual certainty of its release. The light

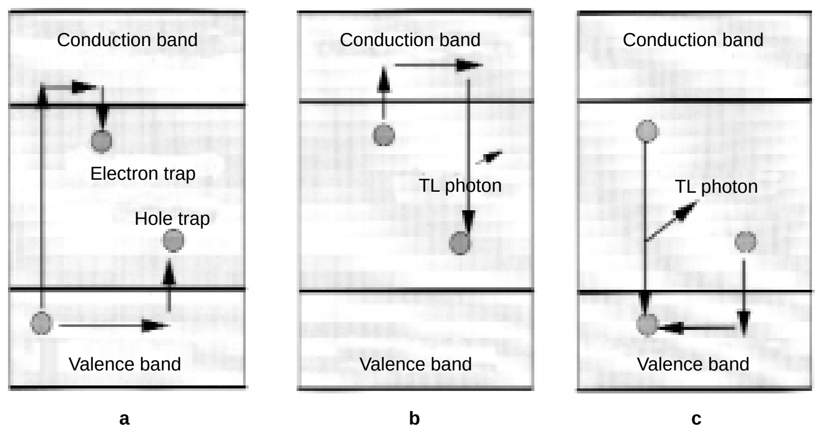

Fig 1 Schematic energy-level diagram of an insulating crystal that exhibits thermoluminescence (TL) related to radiation. (a) Exposure to ionization radiation. (b) Heating: hole trap emitting light. (c) Heating: electron trap emitting light.

emitted (TL) will thus start out weak, go through a maximum, and decrease again to zero. The graph of TL as a function of time or temperature is a glow curve.[19] In most phosphors there are a number of traps, and the glow curve may consist of a number of glow peaks. Of course, if the energy differences are too small or if the heating of the phosphor is too rapid, not all glow peaks will be resolved. If *E* is very small, the trap may be unstable at room temperature, and in that case it can only be observed by keeping the crystal cold during irradiation. If *E* is less than ~ 0.8 eV, many electrons are released at room temperature and common phosphorescence occurs. In a sense, TL can be considered as "frozen-in" phosphorescence that is released upon heating.

TLD is commonly measured through a TLD reader, which is used to detect the light emitted from the TLD chip in a heating unit. For LiF single crystal material, the heating unit is set from 150°C to 240°C, which includes the majority of the light emitted from LiF after irradiation.[22] The amount of total light emission from each sample can be detected to give a quantitative analysis of the radiation dose absorbed by the TLD chips.

Materials and Methods

A combination of four implant systems, four directions of scattered radiation, three locations of bone-implant interfaces, and five samples per group yielded 240 TLD specimens for the experiment groups. An additional 60 TLD specimens were used as the control samples; these specimens were irradiated without dental implants. In total, 300 specimens were included in the study. The treatment procedures and testing conditions are described below.

Measurement Setup. Three root-form cylindrical implant systems were used, based on their different compositions: commercially pure titanium (cpTi) (Nobel Biocare, Göteborg, Sweden); pure titanium coated with hydroxyapatite (HATi) (Dentsply, Encino, CA); and a Ti-6A1-4V implant system (Minimatic Implant Technology, Boca Raton, FL). Two cylindrical screw-type implants from each system (3.75 mm in diameter and 16 mm in length) were surgically placed in one side of an artificial mandible that simulates the bone density of an actual mandible. (Radiation Measurement, Middletown, WI). Each implant was carefully placed so that the distal surface of the first implant was separated from the mesial surface of the second implant by a distance of 6 mm. Troughs measuring $3 \times 3 \times 4$ were created on the mesial, distal, buccal, and lingual aspects of each implant to receive LiF TLD chips (Harshaw Chemical, Solon, OH) and bone substitute blocks (Radiation Measurement).

The $3 \times 3 \times 1$ mm LiF TLD chips were placed in the troughs against the implants in mesial, distal, buccal, and lingual directions to ensure a metal-TLD contact. The $3 \times 3 \times 1$ mm machine-cut bone substitutes, which have the same density as human bone (1.78 g/cm^3), were laid against the TLD chips. This sequence was repeated until all the spaces in the mandibular troughs were filled with the TLD chips

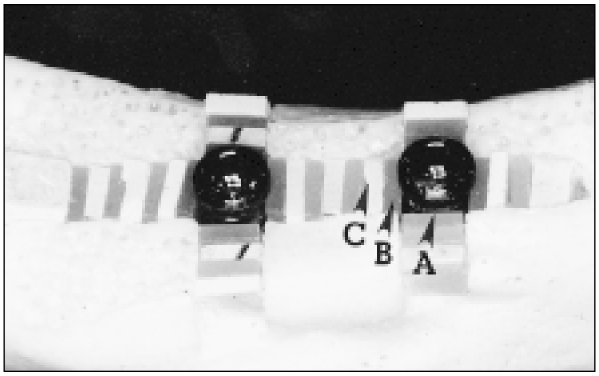

Fig 2 Mandibular assembly for measurement of scattered radiation: A = implant cylinder; B = TLD chip; C = bone-substitute block.

and the bone substitute material. The geometric configuration of the assembly is illustrated in Fig 2. TLD chips function as a radiation detector to measure the relative ionization dose at the bone-implant interfaces. The purpose of TLD chips placed between two implants is to evaluate any cumulative effect of scattered radiation from both implants. For the high gold content transmandibular implant (TMI) system (82% gold, 10% copper, 6% silver), (Biomet, Jacksonville, FL), four transmandibular posts (3.5 mm in diameter, 16 mm in length) were stabilized by a mandibular plate. The TLD chips for the TMI system were placed in the same locations and directions as described for the cylindrical implants. TLD chips and bone substitute materials were also placed in an artificial mandible without implants. This group served as the control to provide a baseline for comparison.

Each mandibular assembly was carefully placed in a cut-out phantom head (Machlett Laboratory, Springdale, IL) to receive simulated head and neck radiotherapy. A dual 6 MeV and 10 MeV linear accelerator (Siemens, Bensheim, Germany) was used as the radiation source. With a radiation field size of 10 × 10 cm and a 100-cm distance from the radiation source, each mandible, with and without implants, was irradiated to 2 Gy at midplane using a pair-opposed bilateral field.

All the irradiated mandibles were disassembled, and the TLD chips were stored at room temperature for 24 hours before measurements were performed. The purpose of this waiting time was to exclude the unstable low-temperature peak emission from the TLD, which changed with time. Each TLD chip was placed in a calibrated TLD reader, which quickly heated the TLD chip from room temperature to 240°C. All light emitted from the TLD chip between 150°C and 240°C was collected by a sensor and converted to electric charges. The amount of emitted light is a measure of the relative dose received by the TLD. A relative comparison of TLD doses from the control and the experimental groups would indicate the level of scattered radiation absorbed by the TLD chips. Each group was measured five times by replacing the TLD chips after they were irradiated under the simulated radiotherapy condition.

Statistical Evaluation. Five specimens were used for each of 60 groups with varied combinations of implant materials, locations, and distances from bone-implant interfaces. Data were first analyzed by a three-way analysis of variance (ANOVA) to evaluate the main effects and two- and three-factor interactions of material distance. Bonferroni Correction and Duncan's test were used for multiple comparison to locate the significant difference. All hypothesis testing was conducted at the significance level of 5%.

Results

The results of the scattered radiation measurements with various materials, locations, and interface distances are presented in Table 1. Analysis of variance was done using the following factors: material (five levels), location (four levels), and distance (three levels). There were five samples for each group of the $5 \times 4 \times 3 = 60$ cells, resulting in 300 observations overall. Table 2 shows the results of ANOVA on the dependent variable TLD. Main effects were significant for material ($P < .001$) and distance ($P < .001$), but not for locations. Two-way interactions were significant for material × distance ($P < .01$), and for material × location ($P < .01$). The three-way interaction of material × distance × location was not significant.

Table 3 shows the means and standard deviations for material × distance. Comparisons were made using a Bonferroni Correction for the degree of freedom. In terms of materials, gold had the highest TLD ($P < .01$). The relative ionization from scattered radiation from CpTi was significantly higher than that of HATi ($P < .01$). The Ti-6A1-4V implants had a higher TLD than the control ($P < .01$), but was not significantly different from HATi. In terms of distances, the mean TLD at 1 mm was lower than that at 0 mm ($P < .001$). The mean TLD at 2 mm and 1 mm did not differ significantly.

Since the main effect of location was insignificant, two-way ANOVA was used to examine the interaction of implant materials and distances. Table 4 presents a summary of the statistical analysis. Table 5 is Duncan's grouping for implant materials and distances. Figure 3 is the relative dose enhancement of various implant materials at bone-implant interfaces. Table 6 is the summary of Duncan's grouping in decreasing order of dose enhancement at bone-implant interfaces. A vertical line represents groups with no statistical differences.

Discussion

Radiotherapy in the head and neck region is often associated with complications, including soft and hard tissue necrosis. The relationship between tissue necrosis and radiation dose has been well recognized. In most instances, the increase in dose caused by scattered radiation of high-energy photons and electrons at tissue-metal interfaces is an undesired complication of the treatment plan.[23–25] Therefore, because of the altered dose distribution caused by scattering from implants or other biomaterials, the amount of radiation dosage to be delivered to the radiation field may need modification.

The results of this study indicate that forwardscatter radiation was not a concern. There are two possible explanations for this. In this study, samples were irradiated by bilateral beams, which may cause even exposure of radiation on both buccal and lingual directions around the implants. Therefore, the amount of measured radiation doses were not statistically different on the buccal and lingual aspects of the dental implants. Bilateral irradiation was used to simulate most clinical situations. The second possible explanation is that the intensity of a transmitted beam after passing through a known thickness can be theoreti-

Table 1 Means and Standard Deviations of Ionization Dose of Implant Materials, Locations, and Directions

Variable	Count	Mean (nanocoulomb)	Standard deviation
Material			
CpTi	60	1.457	0.053
TiHA	60	1.438	0.024
Ti-6A1-4V	60	1.445	0.050
Au-Ag-Cu	60	1.492	0.073
Control	60	1.431	0.024
Location			
Mesial	75	1.460	0.050
Distal	75	1.446	0.056
Buccal	75	1.454	0.058
Lingual	75	1.452	0.054
Distance (mm)			
0	100	1.493	0.062
1	100	1.437	0.039
2	100	1.429	0.035

Table 2 Summary of Three-Way Analysis of Variance for Thermoluminescent Densitometry

Variable	DF†	F value	*P* value
Material	4	28.08	< .001
Location	3	1.93	NS*
Material × location	12	2.71	< .01
Distance	2	101.20	< .001
Material × distance	8	16.64	< .001
Location × distance	6	1.98	NS
Material × location × distance	24	0.80	NS

Error mean square = 0.0012.
*NS = not significant.
†DF = degrees of freedom.

Table 3 Means (and Standard Deviations) of Thermoluminescent Densitometry by Material and Distance*

	Distance (mm)			
Material	0	1	2	Total
TMI† (Au-Ag-Cu)	1.583 (0.036)	1.466 (0.034)	1.432 (0.032)	1.492 (0.034)
Pure titanium	1.502 (0.0037)	1.432 (0.030)	1.440 (0.040)	1.457 (0.036)
Ti-6A1-4V	1.483 (0.049)	1.432 (0.044)	1.422 (0.030)	1.446 (0.041)
Ti + HA coating	1.473 (0.029)	1.422 (0.026)	1.417 (0.036)	1.439 (0.030)
Control	1.421 (0.049)	1.439 (0.028)	1.435 (0.027)	1.432 (0.035)
Total	1.493 (0.040)	1.437 (0.032)	1.429 (0.033)	

*Unit = nanocoulomb.
†TMI = transmandibular implant system.

Table 4 Statistical Summary of Two-Way Analysis of Variance (Material × Distance)

Source	DF	ANOVA SS*	F value	*P* value
Implant material	4	0.1135	22.02	< .001
Distance	2	0.2761	107.12	< .001
Implant material × distance	8	0.1304	12.65	< .001
Error	285	0.3673		
Corrected total	299	0.8873		

*SS = sum of squares.

Table 5 Summary of Main Effects by Implant Material and Distance

Duncan grouping*	N	Material
A	60	TMI gold content
B	60	Pure Ti implant
BC	60	Ti-6A1-4V implant
CD	60	Ti coated with HA implant
D	60	Control
Duncan grouping	**N**	**Distance (mm)**
A	100	0
B	100	1
B	100	2

*Homogenous groups have the same alphabetic letter and align vertically.

Table 6 Duncan's Multiple Range Analysis

Duncan grouping*	N	Material × distance (mm)
A	20	TMI/0
B	20	CpTi/0
BC	20	Ti-6A1-4V/0
C	20	HATi/0
CD	20	Control/0
D	20	TMI/1
DE	20	Control/1
E	20	CpTi/2
E	20	CpTi/1
E	20	Ti-6A1-4V/1
E	20	Control/2
E	20	Ti-6A1-4V/2
E	20	HATi/1
E	20	TMI/2
E	20	HATi/2

*Homogenous groups have the same alphabetic letter and align vertically.

cally calculated. The authors' calculations have shown that dose enhancement from forwardscattering is not a clinical issue.

At the bone-implant interface, the amount of scattered radiation ranged from 10% to 15% with TMI cylindrical implants, which is much less than the results obtained in previous work from a flat disk surface (35 to 46% backscattering).[18] Cylindrical cpTi and Ti-6A1-4V implants demonstrated a similar scattering pattern and no statistical differences. The average dose enhancement was 5.7% for cpTi implants and 4.4% for Ti-6A1-4V implants at the bone-implant interface. These results represent a 65 to 69% reduction in the amount of scattering measured from the flat implant material disks. This phenomenon can probably be attributed to the different sizes and configurations of the samples used in the present study. Interestingly, Ti implants coated with hydroxyapatite were not significantly different from the control group. Coating titanium implants with hydroxyapatite may therefore be a desirable procedure from a radiotherapy point of view.

At 1 mm from the bone-implant interface, dose enhancement from the four implant systems ranged from 0.5% to 2.4%, which is minute and clinically negligible. At 2 mm from the bone-implant interface, dose enhancement from the four implant systems ranged from 0.2% to 0.4%, which was not a clinical concern. When clinicians place a root-form implant adjacent to another implant in a patient's jaw, 6 mm of mesiodistal separation of the two implants is required. The midpoint between the two implants would be 3 mm from the bone-implant interface. On the basis of this study, scattering between two cylindric implants from head and neck radiotherapy would not be of great concern.

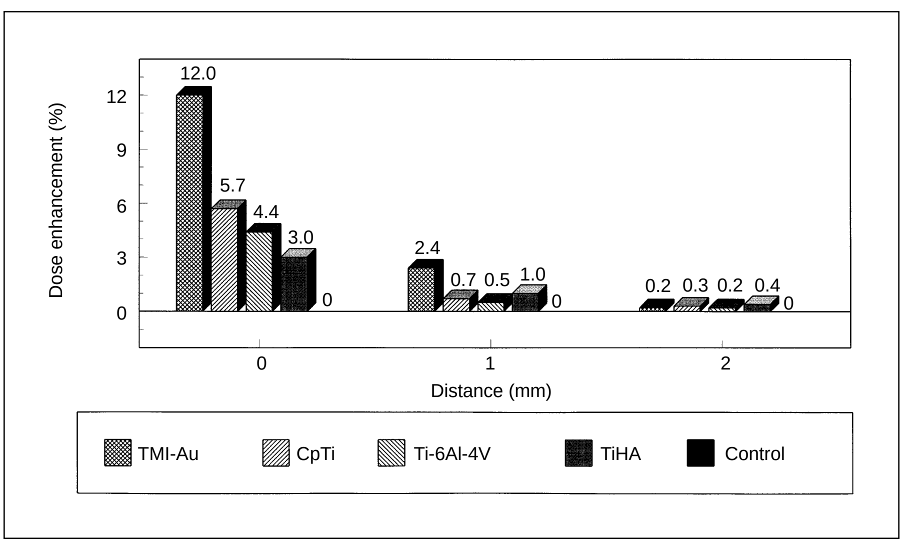

Fig 3 Relative dose enhancement with different implant materials at bone-implant interfaces.

Conclusions

Four currently used dental implant systems consisting of pure Ti, Ti-6A1-4V alloy, titanium coated with hydroxyapatite, and high gold content materials were investigated to determine the level of scattered radiation at bone-implant interfaces by 6 MeV x-ray. Under the conditions of the study, the following conclusions were drawn:

1. The greatest amount of scattered radiation for all studied implant systems occurred at bone-implant interfaces. There was no significant difference in scattering at 1 mm and at 2 mm from the bone-implant interface for all the implant systems studied.
2. The high gold content transmandibular implant system had a significantly higher dose enhancement than the other groups tested.
3. Titanium implants coated with hydroxyapatite were statistically indistinguishable from the control group, which had no implants.
4. Dose enhancement from scattered radiation in mesial, lingual, distal, and buccal directions was not significantly different.

References

1. American Association of Maxillofacial Surgeons. Dental implants. AAOMS Surgical Update 1992;14:3–9.
2. Dreizen SM, Dale TE, Drane JB, Brown LR. Oral complications of cancer therapy. Postgrad Med 1977;61:85–92.
3. Rothwell BR. Prevention and treatment of the orofacial complications of radiotherapy. J Am Dent Assoc 1987;114:316–322.
4. Meyer IR. Infectious disease and osteoradionecrosis of the jaw. J Oral Surg 1984;16:819–827.
5. Wang CC. Radiation therapy for head and neck neoplasms. 2nd ed. Chicago: Year Book Medical Publishing 1989:113–119.
6. Marx RE, Johnson RD. Studies in the radiobiology of osteoradionecrosis and their significance. Oral Surg 1987;64:379–390.
7. Murray CG, Herson J, Daly TE, Zimmerman ST. Radiation necrosis of the mandible: A 10-year study. Part I. Factors influencing the onset of necrosis. Int J Radiat Oncol Biol Phys 1980;6:543–548.
8. Murray CG, Herson J, Daly TE, Zimmerman ST. Radiation necrosis of the mandible: A 10-year study. Part II. Dental factors, onset, duration and management of necrosis. Int J Radiat Oncol Biol Phys 1980;6:549–535.
9. Beumer J, Harrison R, Sanders B, Kurrasch M. Osteoradionecrosis: Predisposing factors and outcomes of therapy. Head Neck Surg 1984;6:819–827.
10. Saunders JF, Peter BG. Backscattering from metals in superficial therapy with high energy electron. Br J Radiol 1974;47:467–470.
11. Weatherburn H, McMillian KT, Stedeford G. Physical measurements and clinical observations on the backscatter of 10 MV electrons from lead shielding. Br J Radiol 1975;48:229–232.
12. Farahani M, Eichmiller FC, McLaughlin WL. Measurement of absorbed doses near metal and material interfaces irradiated by X and gamma ray beams. Phys Med Biol 1990;35:369–385.
13. Thambi V, Murthy AD, Alder G. Dose perturbations resulting from gold fillings in patients with head and neck cancers. Int J Radiat Oncol Biol Phys 1979;5:581–588.
14. Farman AG, Sharma S, George DL, Wilson D, Didd D, Figa R. Backscattering from dental restorations and splint materials during therapeutic radiation. Radiology 1985;156:523–527.
15. Gagnon WF, Gundiff JH. Dose enhancement from backscattered radiation at tissue-metal interfaces irradiated with high energy electrons. Br J Radiol 1980;53:466–472.
16. Hazuka MB, Ibbot SG, Kinzie JJ. Hip prostheses during pelvic irradiation: Effects and corrections. Int J Radiat Oncol Biol Phys 1988;14:1311–1317.
17. Mian TA, VanPutten MC, Kramer DC, Jacob RF, Boyer AL. Backscatter radiation at bone-titanium interface from high-energy x and gamma rays. Int J Radiat Oncol Biol Phys 1988;14:1943–1948.
18. Wang RR, Pillai K, Jones PK. In vitro backscattering from implant materials during radiotherapy. J Prosthet Dent 1996;75:626–632.
19. Cameron JR, Suntharalingram N, Kenney G. Thermoluminescent Dosimetry. Madison: Univ of Wisconsin Press, 1968:30–51.
20. Kron T. Thermoluminescent dosimetry and it applications in medicine. Part 1: Physics, materials and equipment. Australas Phys Eng Sci Med 1994;17:175–199.
21. Kron T. Thermoluminescent dosimetry and it applications in medicine. Part 2: History and applications. Australas Phys Eng Sci Med 1995;18:1–25.
22. Wood JJ, Mayles WP. Factors affecting the precision of TLD dose measurements using an automatic TLD reader. Phys Med Biol 1995;40:309–413.
23. Mondalek PM, Feyad JM. Prostate adenocarcinoma: Treatment planning considerations with a hip prosthesis. Clin Orthop 1984;83:4–11.
24. Hudson FR, Crawley MT, Samarasekera M. Radiotherapy treatment planning for patient fitted with prostheses. Br J Radiol 1988;61:603–608.
25. Rao K. Dose delivered by secondary electron radiated by metallic objects implanted in human tissue during radiotherapy using high energy photons. Acta Med Pol 1989;30:147–166.